Electronic Supplementary Material (ESI) for Journal of Materials Chemistry A.

Supporting information

A highly sensitive and ultra-stretchable zwitterionic liquid hydrogel-based sensor as anti-freezing ionic skin

Yabin Zhang[a#], Tianyu Li[a#], Luyang Miao[a], Prabhleen Kaur[c], Shaojie Men[d], Qiong Wang[e], Xin Gong[a], Yuelin Fang[b], Congcong Zhai[a], Shuxiang Zhang[a], Luqing Zhang[a*], Lei Ye[b*]

[a] *Shandong Provincial Key Laboratory of Fluorine Chemistry and Chemical Materials, School of Chemistry and Chemical Engineering, University of Jinan, Jinan 250022, China*

[b] *Department of Pharmaceutics, Key Laboratory of Chemical Biology (Ministry of Education), School of Pharmaceutical Sciences, Shandong University, Jinan, Shandong 250012, China*

[c] *Department of Chemical Engineering, University of Washington, Seattle, Washington 98195, United States*

[d] *School of Information Science & Engineering and Shandong Provincial Key Laboratory of Laser Technology and Application, Shandong University, Qingdao 266237, China*

[e] *College of Chemistry, Shandong Normal University, Jinan 250014, China*

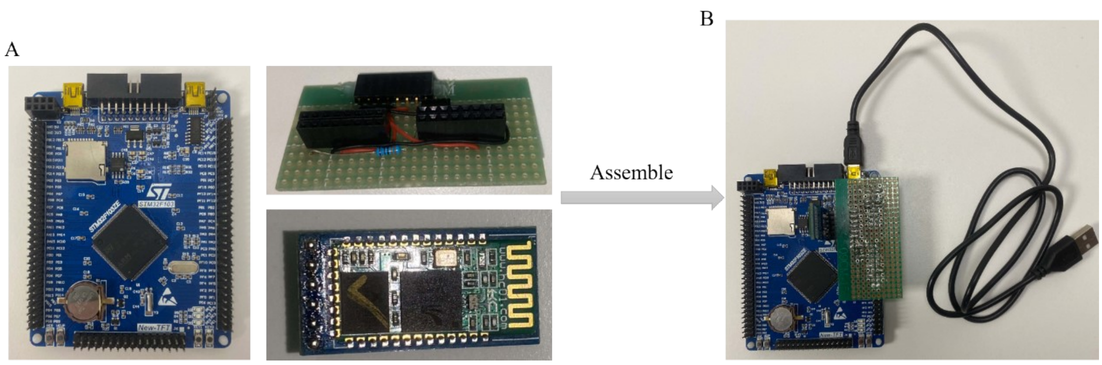

Figure S1. The demonstration of wireless sensor system. (A) Components of the wireless sensor system for the collection, conversion and wireless transmission of human motion signals. (B) The assembled wireless sensor system.

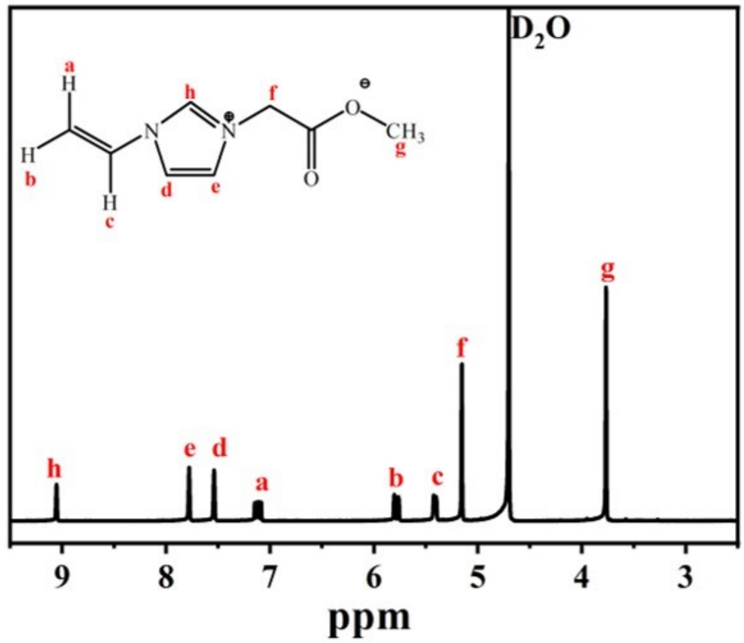

Figure S2 The NMR spectrum of 1-vinyl-3-methoxycarbonyl-imidazole.

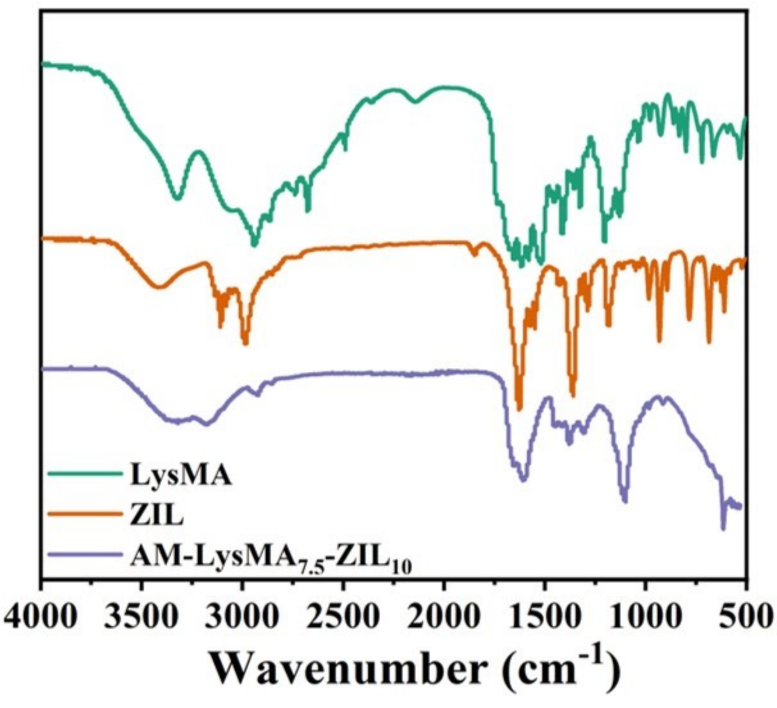

Figure S3 The FT-IR spectra of the LysMA, ZIL and AM-LysMA-ZIL polymer.

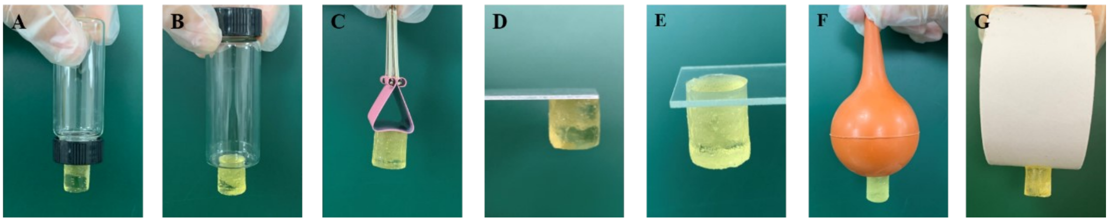

Figure S4 The adhesion evaluation of the hydrogel by bearing its weight with different surfaces: (A) plastic, (B) glass, (C) stainless steel, (D) aluminum plate, (E) glass, (F) rubber, (G) paper.

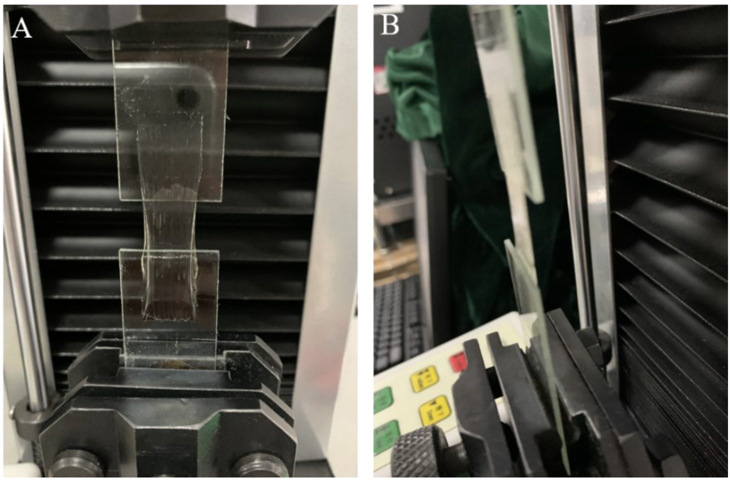

Figure S5 The front (A) and side (B) photos of the lap shear test.

Figure S6 Quantitative observation of the stretchability of Am-ZIL_{10}-$LysMA_{7.5}$ hydrogel against the ruler.

Figure S7 The digital photographs show the self-recovery process.

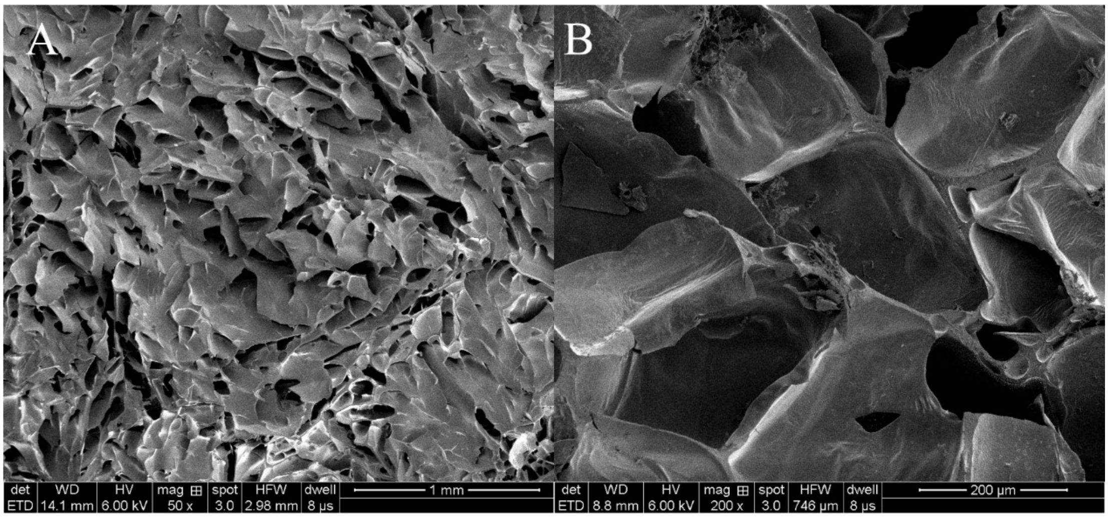

Figure S8 SEM images of the hydrogel at different magnifications

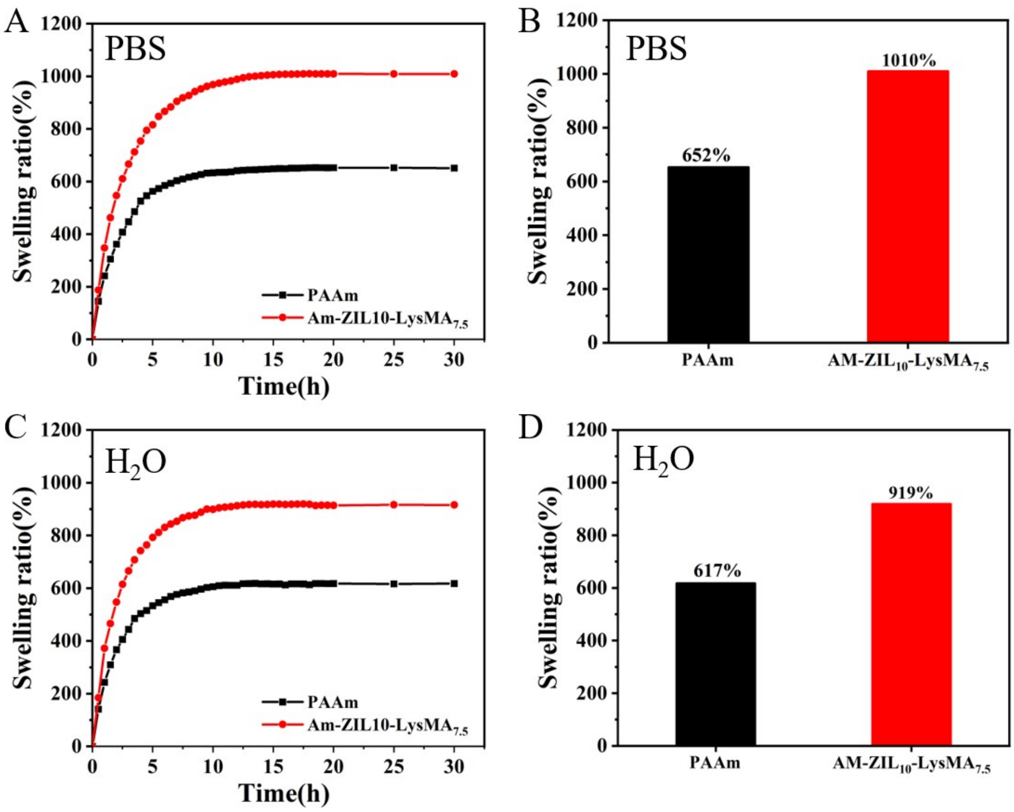

Figure S9 Swelling properties of the PAAm and Am-ZIL_{10}-$LysMA_{7.5}$ hydrogels in different media. Swelling kinetics curves (A, C) and equilibrium swelling ratios (B, D) of hydrogels in PBS and DI water, respectively.

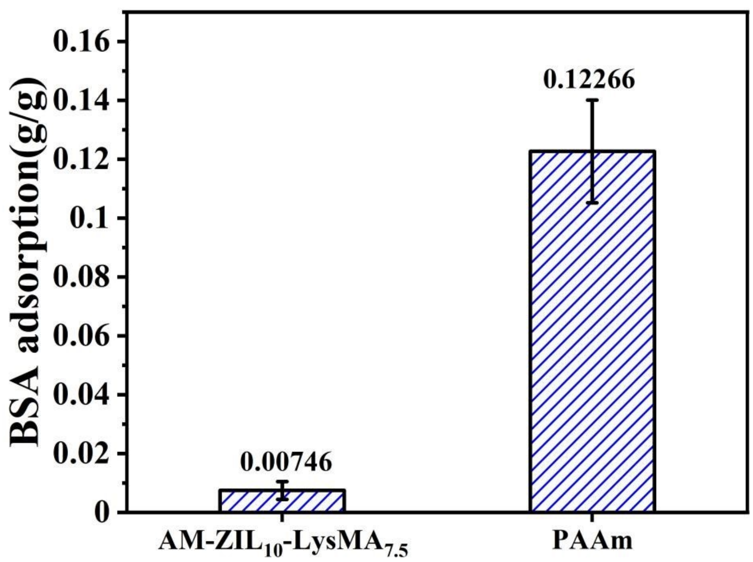

Figure S10 Protein adsorption of the PAAm and Am-ZIL_{10}-$LysMA_{7.5}$ hydrogels against BSA.

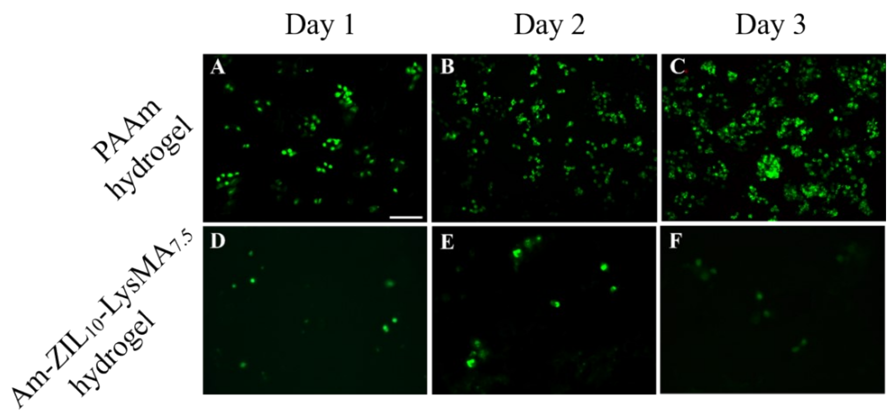

Figure S11 Cell adhesion on PAAm and Am-ZIL$_{10}$-LysMA$_{7.5}$ hydrogels with HepG2 cells at different periods of time. Bar:100μm.

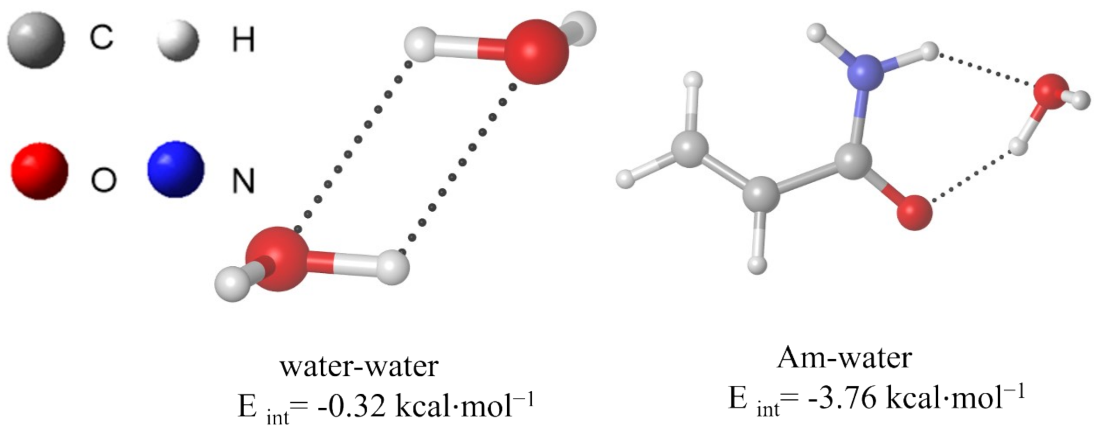

Figure S12 Molecular simulations of the interaction energy between water-water and Am-water.

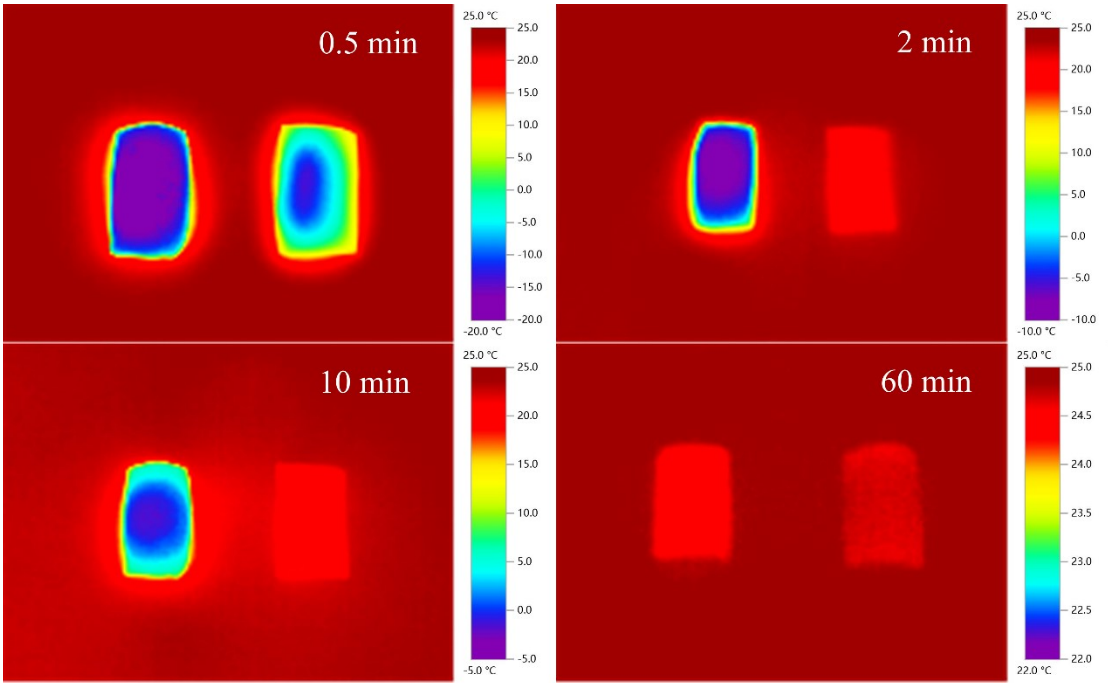

Figure S13 Infrared thermography images of PAAm and Am-ZIL_{10}-$LysMA_{7.5}$ hydrogel returning from -20 ◦C to room temperature.

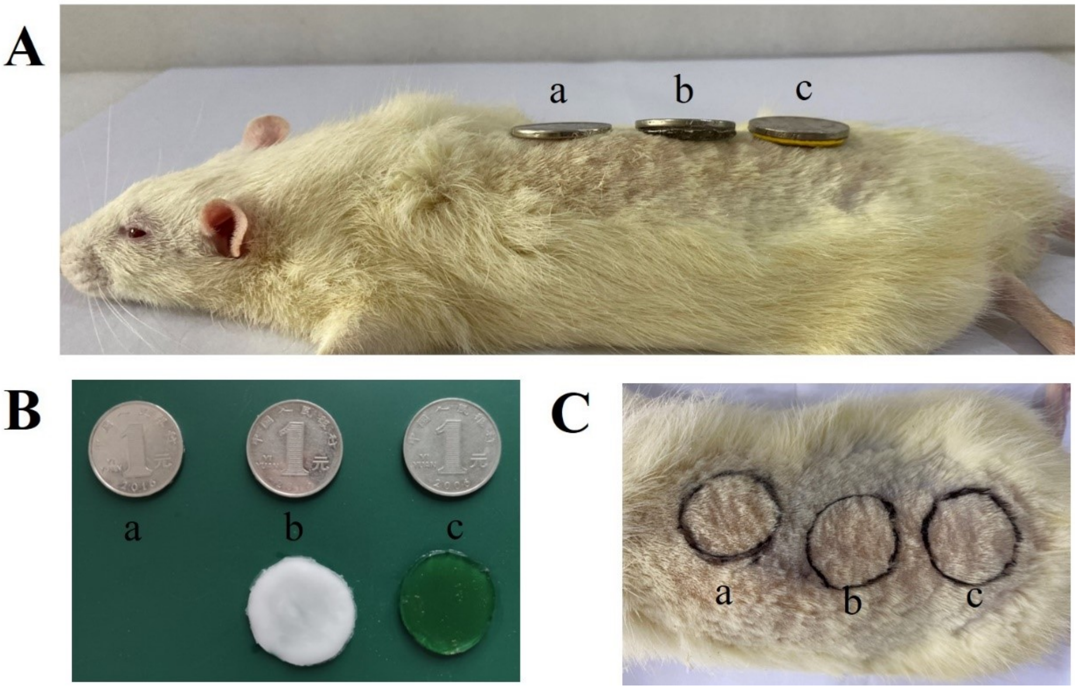

Figure S14 Frosbite experiments on rats' back skin to exhibit the cold tolerance of PAAm and Am-ZIL_{10}-$LysMA_{7.5}$ hydrogels. (A) Schematic diagram of frostbite model. Extremely cold coins attachted on the (a) bare skin, (b) PAAm hydrogel and (c) Am-ZIL_{10}-$LysMA_{7.5}$ hydrogel. Photos of (B) skin, (C) cold coins and hydrogel after covering the cold coin for 30s.

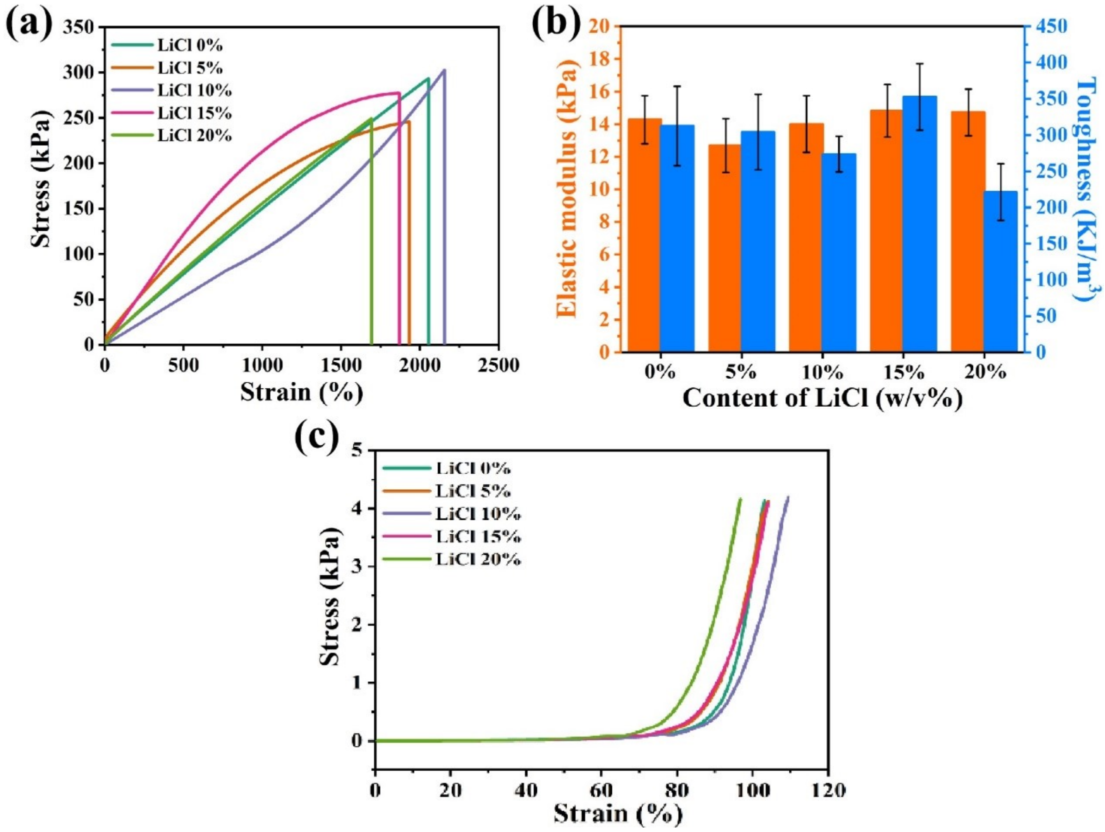

Figure S15 The mechanical changes of the hydrogels with different LiCl concentrations. (A) Tensile stress-strain curves; (B)Toughness stress; (C)Compressive stress-strain curves.

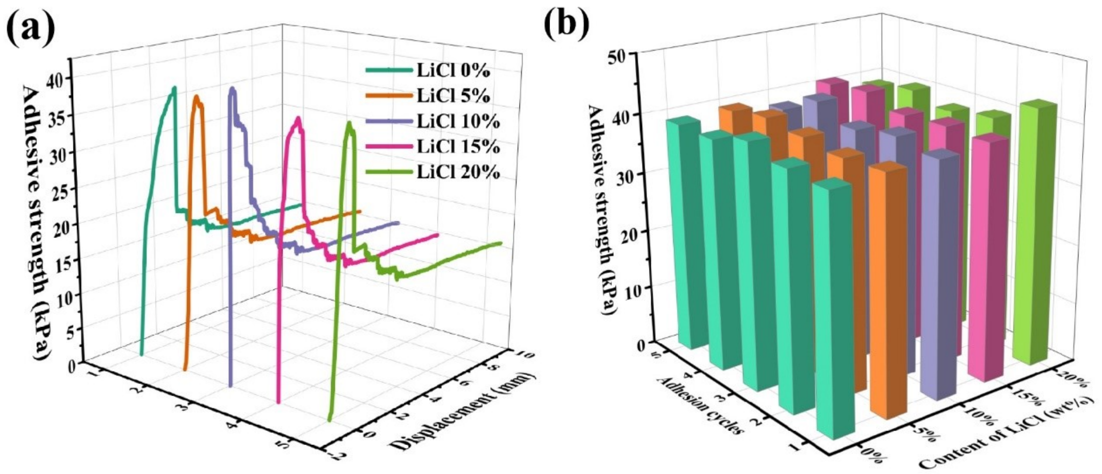

Figure S16 The adhesive strength changes of the hydrogels with different LiCl concentrations. (A) the adhesive strength curve; (B) the adhesive strength of the hydrogel with five repeat tests.

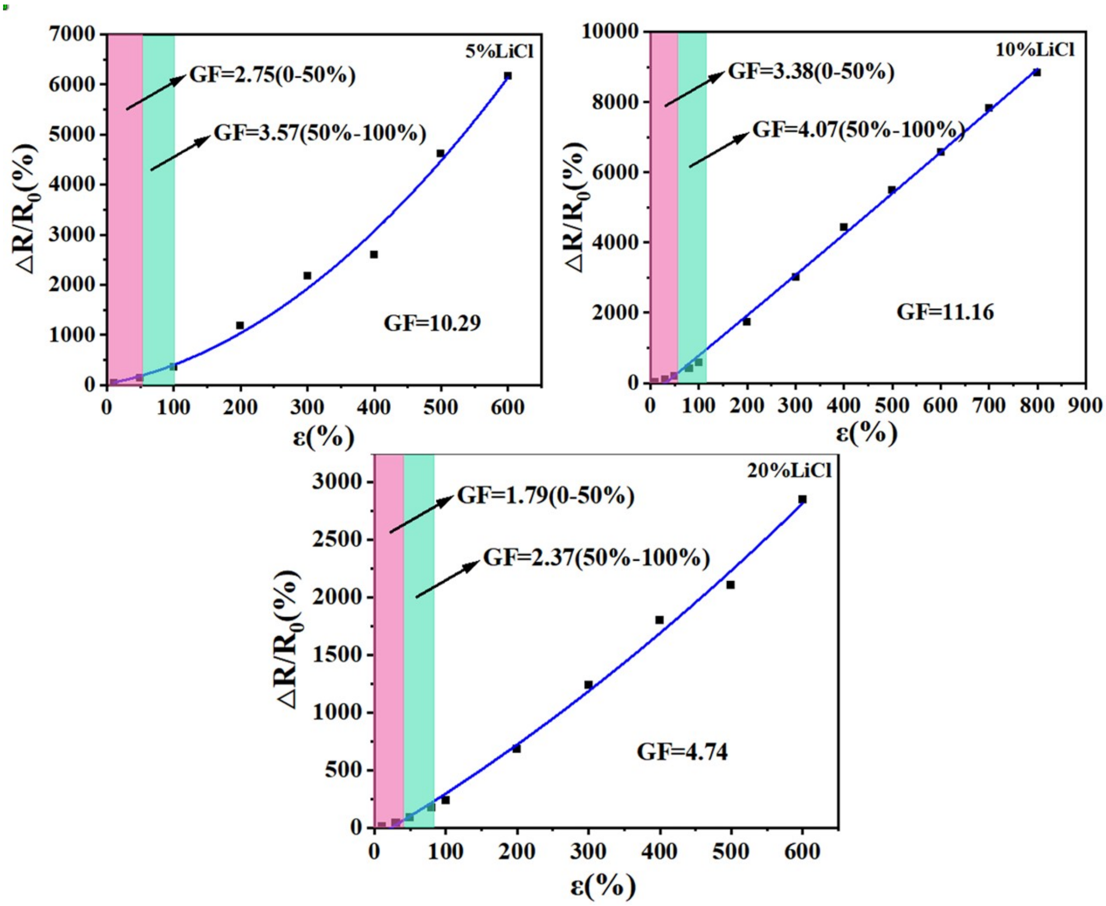

Figure S17 The GF values of Am-ZIL$_{10}$-LysMA$_{7.5}$-LiCl hydrogel with different LiCl content under 0-1000% strain.

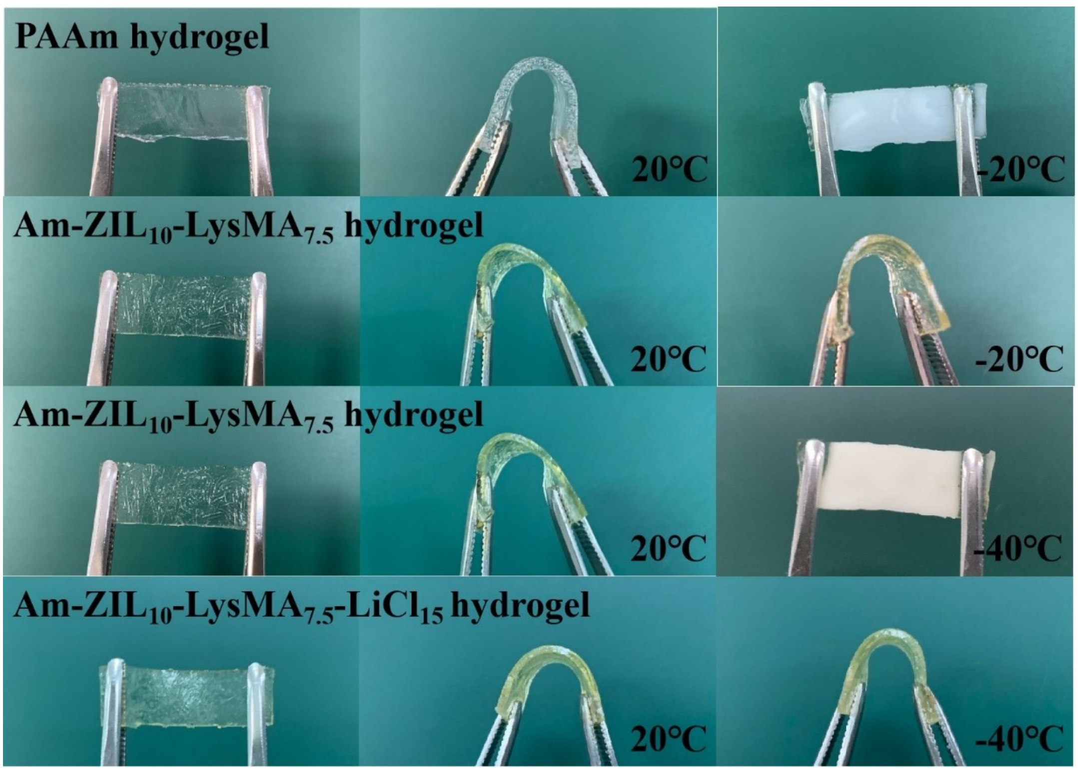

Figure S18 The state of the PAAm, Am-ZIL_{10}-$LysMA_{7.5}$, Am-ZIL_{10}-$LysMA_{7.5}$-$LiCl_{15}$ hydrogels at different temperatures.

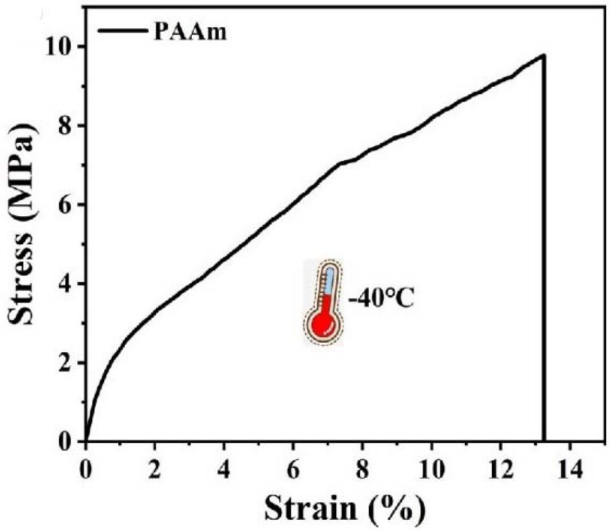

Figure S19 Tensile stress-strain curves of the PAAm hydrogel at -40 °C.

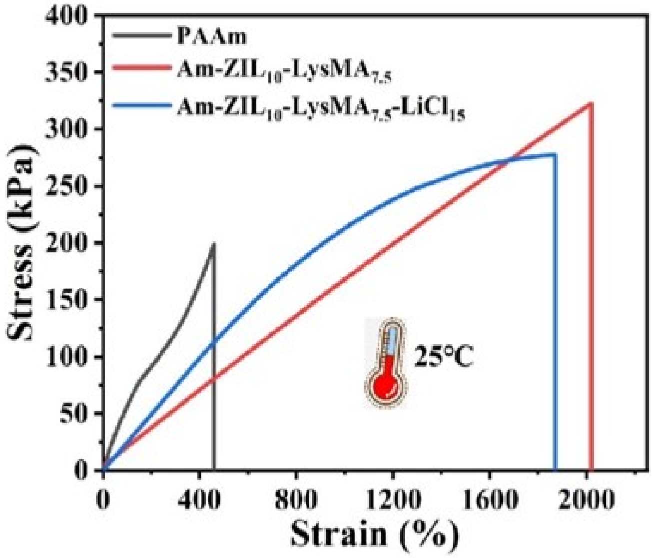

Figure S20 Tensile stress-strain curves of the PAAm, Am-ZIL_{10}-$LysMA_{7.5}$, Am-ZIL_{10}-$LysMA_{7.5}$-$LiCl_{15}$ hydrogels at 25 °C.

Table S1 Summary of different types of hydrogel-based strain sensors.

Composition	GF (tensile strain）	Transparency	Stretchability	Conductivity (ms·cm^{-1}）	Anti-freezing	Adhesion	Ref
PAAm/Agar/LiCl	1.8 (1100%)	Transparent	1680%	−	−	−	[46]
OIC	2.86 (＞60%)	Transparent	1219%	7.90 × 10$^{−1}$	-100 ºC	−	[47]
OEGMA-based gels	2.23 (600%)	Transparent	1600%	3.32 × 10$^{−1}$	-20 ºC	−	[48]
TA@HAP NWs-PVA	2.84 (350%)	Transparent	480%	−	−	−	[49]
CCH	0.84 (200%)	Transparent	217%	−	-27.8 ºC	−	[50]
PAAm/Cs-c-MWCNT	3.2 (100%)	Opaque	2761%	−	−	33N/m	[51]
Ca-GG/PAAm-ZP	4.86 (500%)	Transparent	1800%	−	-40 ºC	8.12Kpa	[2]
Carbon nanotube/PVA	1.51 (1000%)	Opaque	1000%	−	−	−	[52]
PAAFC/LiCl	2.32 (900%)	Transparent	1200%	39.6	−	−	[53]
PACG/MXene	3.93 (600%)	Opaque	~1000%	13.4	-20 ºC	−	[54]
Agar/Acrylic acid/Fe^{3+}	0.348 (700%)	Transparent	3174%	−	−	−	[55]
CMC/PAAm/LiCl	3.15 (1000%)	Transparent	1363%	−	−	−	[56]
PAAm/ZIL/LysMA	6.42 (800%)	Transparent	2060%	24.8	-20 ºC	39.91Kpa	This work
PAAm/ZIL/LysMA/LiCl	14.96 (＞500%)	Transparent	2600%	81	-40 ºC	77Kpa	This work

Noted: In this table, **PAAm, OIC, OEGMA, TA@HAP NWs, PVA, CCH, Cs, c-MWCNT, GG, ZP, CMC** are the abbreviations of polyacrylamide, organogel ionic conductor, oligo(ethylene glycol) methacrylate, tannic acid-coated hydroxyapatite nanowires, polyvinyl alcohol, ionic conductive cellulose hydrogel, chitosan, carboxyl-functionalized multi-walled carbon nanotubes, gellan gum, zwitterionic proline, carboxymethylcellulose. **PAAFC/LiCl:** The hydrogel was generated from a facile one-pot free radical polymerization process of acrylamide (AM), and 2-aminoethyl acrylamide hydrochloride (AEAM), with the presence of carboxymodified multiwall carbon nanotubes (MWCNTs) and aldehyde-terminated poly(ethylene oxide)-b-poly(propylene oxide)-b-poly(ethylene oxide) (F127-CHO) and LiCl under neutral conditions. **PACG/MXene:** a poly(acrylamide-acrylic acid)/chitosan/MXene hydrogel. “−”means Not mentioned.

Table S2 Summary of performance results of reported stretchable strain sensors

Composition	GF (tensile strain）	Transparency	Stretchability	Conductivity (ms·cm^{-1}）	Anti-freezing	Adhesion	Ref
PAAm/Car/KCl	6 (400%)	Transparent	950%	–	-18 ºC	–	[18]
PAAm/Agar/LiCl	1.8 (1100%)	Transparent	1680%	–	–	–	[46]
CMC/PAAm/LiCl	3.15 (1200%)	Transparent	1363%	–	–	–	[56]
ICEs	6 (200%)	Transparent	1640%	5.28×10^{-2}	−14.4 ºC	–	[58]
TA/SA/PAAm	9.0 (2100%)	Opaque	2100%	–	–	46Kpa	[59]
LM-PDES	2.17 (＞500%)	Transparent	2600%	–	-40 ºC	–	[60]
J-AuNPs@GA /LiCl	0.303(600-800%)	Transparent	~1800%	–	–	Yes	[61]
LiCl-loaded PAA-based organohydrogel	0.32 (300%)	Transparent	~900%	~10	-80 ºC	Yes	[62]
PAAFC/LiCl	2.32 (900%)	Transparent	1200%	39.6	–	–	[53]
PACG/MXene	3.93 (600%)	Opaque	~1000%	13.4	-20 ºC	Yes	[54]
PAAm/ZIL/LysMA/LiCl	14.96 (＞500%)	Transparent	2600%	81	-40 ºC	77Kpa	This work

Noted: In this table, **PAAm, Car, CMC, ICES, TA, SA** are the abbreviations of polyacrylamide, carrageenan, sodium carboxymethylcellulose, liquid-free ionic conductive elastomers, tannic acid and sodium alginate respectively, “–” means Not mentioned.

Table S3 The formulations of Am-ZIL-LysMA hydrogels

Hydrogels	Am (g)	ZIL (g)	LysMA (g)	APS (g)	TMEDA (g)	H_2O (mL)
Am-ZIL$_{10}$-LysMA$_0$(LysMA$_0$)	3.5	1.56	0	0.03	0.016	10
Am-ZIL$_{10}$-LysMA$_{2.5}$(LysMA$_{2.5}$)	3.5	1.56	0.0875	0.03	0.016	10
Am-ZIL$_{10}$-LysMA$_{5.0}$(LysMA$_{5.0}$)	3.5	1.56	0.0175	0.03	0.016	10
Am-ZIL$_{10}$-LysMA$_{7.5}$(LysMA$_{7.5}$)	3.5	1.56	0.2625	0.03	0.016	10
Am-ZIL$_{10}$-LysMA$_{10}$(LysMA$_{10}$)	3.5	1.56	0.3500	0.03	0.016	10

Table S4 The formulations of Am-ZIL-LysMA-LiCl hydrogels

Hydrogels	Am (g)	ZIL (g)	LysMA (g)	APS (g)	TMEDA (g)	H_2O (mL)
Am-ZIL_0-$LysMA_{7.5}$(ZIL_0)	3.5	0	0.2625	0.03	0.016	10
Am-ZIL_5-$LysMA_{7.5}$(ZIL_5)	3.5	0.74	0.2625	0.03	0.016	10
Am-ZIL_{10}-$LysMA_{7.5}$(ZIL_{10})	3.5	1.56	0.2625	0.03	0.016	10
Am-ZIL_{15}-$LysMA_{7.5}$(ZIL_{15})	3.5	2.48	0.2625	0.03	0.016	10

References

[2] Q. Jiao, L. Cao, Z. Zhao, H. Zhang, J. Li, Y. Wei, Zwitterionic Hydrogel with High Transparency, Ultrastretchability, and Remarkable Freezing Resistance for Wearable Strain Sensors, Biomacromolecules, 2021, 22(3),1220-1230.

[18] J. Wu, Z. Wu, X. Lu, S. Han, B.R. Yang, X. Gui, K. Tao, J. Miao, C. Liu, Ultra stretchable and Stable Strain Sensors Based on Antifreezing and Self-Healing Ionic Organohydrogels for Human Motion Monitoring, ACS Appl Mater Interfaces 11(9) (2019) 9405-9414.

[32] B. Yang, W. Yuan, Highly Stretchable and Transparent Double-Network Hydrogel Ionic Conductors as Flexible Thermal-Mechanical Dual Sensors and Electroluminescent Devices, ACS Appl Mater Interfaces 11(18) (2019) 16765-16775.

[42] T.X. Zhua， Y. Cheng，C.Y. Cao，J. J. Mao，L.Q. Li，J. Y. Huang，S. W. Gao, X. L. Dong，Z. Chen，Y. K. Lai, A semi-interpenetrating network ionic hydrogel for strain sensing with high sensitivity, large strain range, and stable cycle performance, Chem Eng J 385 (2021).

[43] B. Yiming, Y. Han, Z. Han, X. Zhang, Y. Li, W. Lian, M. Zhang, J. Yin, T. Sun, Z. Wu, T. Li, J. Fu, Z. Jia, S. Qu, A Mechanically Robust and Versatile Liquid-Free Ionic Conductive Elastomer, Adv Mater 33(11) (2021) e2006111.

[44] H. Qiao, P. Qi, X. Zhang, L. Wang, Y. Tan, Z. Luan, Y. Xia, Y. Li, K. Sui, Multiple Weak H-Bonds Lead to Highly Sensitive, Stretchable, Self-Adhesive, and Self-Healing Ionic Sensors, ACS Appl Mater Interfaces 11(8) (2019) 7755-7763.

[45] Z.L. Ming Wang, Xiaolin Jin, Taolin Sun, Hongchen Liu, and Haisong Qi, Multifunctional Liquid-Free Ionic Conductive Elastomer Fabricated by Liquid Metal Induced Polymerization, Adv. Funct. Mater. (2021).

[46] B. Yang, W. Yuan, Highly Stretchable and Transparent Double-Network Hydrogel Ionic Conductors as Flexible Thermal-Mechanical Dual Sensors and Electroluminescent Devices, Acs. Appl. Mater. Inter., 2019, 11(18), 16765-16775.

[47] Y.Y. Gao, L. Shi, S.Y. Lu, T.X. Zhu, X.Y. Da, Y.H. Li, H.T. Bu, G.X. Gao, S.J. Ding, Highly Stretchable Organogel Ionic Conductors with Extreme-Temperature Tolerance, Chem. Mater., 2019, 31(9), 3257-3264.

[48] J. Kong, J.X. Zhang, Y.F. Wang, W. Qi, M.M. Huang, R.X. Su, Z.M. He, Bioinspired

Fluorescent Peptidyl Nanoparticles with Rainbow Colors, Acs. Appl. Mater. Inter., 2020, 12(28), 31830-31841.

[49] J. Wen, J. Tang, H.M. Ning, N. Hu, Y.Y. Zhu, Y.K. Gong, C.H. Xu, Q.N. Zhao, X.P. Jiang, X.L. Hu, L. Lei, D. Wu, T. Huang, Multifunctional Ionic Skin with Sensing, UV-Filtering, Water-Retaining, and Anti-Freezing Capabilities, Adv. Funct. Mater., 2021, 31(21), 2011176.

[50] Y. Wang, L. Zhang, A. Lu, Transparent, Antifreezing, Ionic Conductive Cellulose Hydrogel with Stable Sensitivity at Subzero Temperature, Acs. Appl. Mater. Inter., 2019, 11(44), 41710-41716.

[51] S. Xia, S.X. Song, F. Jia, G.H. Gao, A Flexible, Adhesive and Self-healable Hydrogel-Based Wearable Strain Sensor for Human Motion and Physiological Signal Monitoring, J. Mater. Chem. B, 2019, 7(30), 4638-4648.

[52] G.F. Cai, J.X. Wang, K. Qian, J.W. Chen, S.H. Li, P.S. Lee, Extremely Stretchable Strain Sensors Based on Conductive Self-healing Dynamic Cross-links Hydrogels for Human-motion Detection, Adv. Sci., 2017, 4(2), 1600190.

[53] M. Wu, J.S. Chen, Y.H. Ma, B. Yan, M.F. Pan, Q.Y Peng, W.D. Wang, L.B. Han, J.F. Liu, H.B. Zeng, Ultra Elastic, Stretchable, Self-healing Conductive Hydrogels with Tunable Optical Properties for Highly Sensitive Soft Electronic Sensors, J. Mater. Chem. A, 2020, 8(46), 24718-24733.

[54] S.N. Li, Z.R. Yu, B.F. Guo, K.Y. Guo, Y. Li, L.X Gong, L. Zhao, J. Bae, L.C. Tang, Environmentally Stable, Mechanically Flexible, Self-adhesive, and Electrically Conductive Ti_3C_2TX MXene Hydrogels for Wide-temperature Strain Sensing, Nano Energy, 2021, 90 106502.

[56] T.X. Zhua， Y. Cheng，C.Y. Cao，J. J. Mao，L.Q. Li，J. Y. Huang，S. W. Gao, X. L. Dong，Z. Chen，Y. K. Lai, A Semi-interpenetrating Network Ionic Hydrogel for Strain Sensing with High Sensitivity, Large Strain Range, and Stable Cycle Performance, Chem. Eng. J., 2021, 385,123912.

[58] B. Yiming, Y. Han, Z. Han, X. Zhang, Y. Li, W. Lian, M. Zhang, J. Yin, T. Sun, Z. Wu, T. Li, J. Fu, Z. Jia, S. Qu, A Mechanically Robust and Versatile Liquid-Free Ionic Conductive Elastomer, Adv. Mater., 2021, 33(11), 2006111.

[59] H. Qiao, P. Qi, X. Zhang, L. Wang, Y. Tan, Z. Luan, Y. Xia, Y. Li, K. Sui, Multiple Weak H-Bonds Lead to Highly Sensitive, Stretchable, Self-Adhesive, and Self-Healing Ionic Sensors, Acs. Appl. Mater. Inter., 2019, 11(8), 7755-7763.

[60] M. Wang, Z.B. Lai, X.L. Jin, T.L. Sun, H.C. Liu, H.S. Qi, Multifunctional Liquid-Free Ionic Conductive Elastomer Fabricated by Liquid Metal Induced Polymerization, Adv. Funct. Mater., 2021, 2101957.

[61] X.J. Zhang, Y.C. Zhang, W.L. Zhang, Y. Dai, F. Xia, Gold Nanoparticles-deranged Double Network for Janus Adhesive-tough Hydrogel as Strain Sensor, Chem. Eng. J., 2021, 130447.

[62] Y. Niu, H. Liu, R.Y. He, M.Q. Luo, M.G. Shu, F. Xu, Environmentally Compatible Wearable Electronics Based on Ionically Conductive Organohydrogels for Health Monitoring with Thermal Compatibility, Anti-Dehydration, and Underwater Adhesion. Small, 2021, 2101151.